

# STRAIN RATE-RELATED CHARACTERIZATION OF FATIGUE BEHAVIOR OF GLASS-FIBER-REINFORCED POLYURETHANE

Daniel Huelsbusch, Michael Jamrozy, Selim Mrzljak and Frank Walther

Department of Materials Test Engineering (WPT), TU Dortmund University,  
Baroper Str. 303, D-44227 Dortmund, Germany  
Email: daniel.huelsbusch@tu-dortmund.de, Web Page: <http://www.wpt-info.de>

**Keywords:** Fatigue, Glass-fiber-reinforced polyurethane,  
Hysteresis measurement, Strain rate dependency

## ABSTRACT

Standardization and reproducibility are of utmost importance regarding test methods and material characteristics. In this context, material properties, for example, strain rate dependency, have to be taken into account for defining test parameters. The aim of this study is the characterization of the strain rate-dependent cyclic deformation behavior of glass-fiber-reinforced polyurethane (GFR-PU) through instrumented multiple amplitude tests (MAT). MAT offer the opportunity for resource-efficient estimation of the fatigue properties and are suitable for investigating strain rate dependency since variable stress amplitudes lead to a change in stress rate and thereby strain rate. The test frequency was varied to realize constant stress rate for indirect strain rate adjustment while cyclic loading. The results were compared to MAT with constant frequency representing the conventional test procedure. Hysteresis measurements, i.e. dynamic Young's modulus and loss energy, as well as temperature measurements, were carried out to determine the strain rate specific material behavior and damage processes, respectively.

Measurands show strain rate dependency by significantly reducing the change in temperature and loss energy under adjusted frequency. Particularly, temperature values are reduced by approximately 85%, which indicates an advanced damage state under constant frequency. However, dynamic Young's modulus shows larger drops at a constant frequency, which is paradoxical regarding the relationship of stiffness and strain rate under quasi-static loading. The different developments of measurands values between the two approaches proof the necessity for improved cyclic test methods regarding strain rate to allow reproducible and comparable results. In this context, a method will be explained in the current study showing one opportunity for the combination of stress-controlled testing and steady constant strain rate.

## 1 INTRODUCTION

The EU climate and energy package 2050, with the objective of reducing emissions by 80% below 1990 levels, is one of the biggest challenges for the automobile industry these days. Therefore, new approaches for energy efficiency must be developed. An already well-known approach is represented by lightweight design. In this context, due to their high specific strength and multi-component structure, new polymer composites are ideal for utilization in transportation industries [1]. The successful integration of composites is, among others, currently represented by e.g. BMW i3, which exhibits a framework mostly designed out of fiber-reinforced polymers (FRP).

However, in applications of the automobile industry, cyclic loading occurs and must be considered for structural design, supported by characterizing the material fatigue behavior. Since fatigue investigations imply high time and cost efforts, optimized cyclic test methods must be developed due to the upcoming challenge of constantly reduced product cycle times within the automobile industry. A suitable method for short-term evaluation of fatigue behavior is given in the load increase test (LIT), which allows an estimation of the performance capabilities of metals and composites [2,3]. Regarding the reduced cycle times, the LIT shows great potential for saving an unnecessary amount of effort through estimating performance capabilities, before an in-depth characterization by means of S-N

curves would be needed. In addition, due to increasing utility of polymers and complexity of material structures and components, test methods have to be standardized and must allow reproducible determination of material characteristics. Therefore, the specific material properties have to be considered while defining test parameters. In this context, strain rate dependency represents a central material property, which has an influence on the determined characteristic values in the case of FRP [4,5]. The strain rate dependency for polymers is caused by macromolecule rearrangement and is also called time dependency. A higher strain rate results in a shorter cycle time, which influences the speed of the rearrangement process and thereby the material characteristics. Concerning LIT, the strain rate dependency is a significant factor because the stress amplitude can be varied continuously or stepwise, and thus significant differences in the strain rate can be present. This renders a reproducible evaluation more difficult. Polymers are also influenced by temperature, which correlates with the strain rate and should be recorded as well to understand the trend of the material properties [6,7]. In terms of previous cyclic investigations, several researchers adjust the test frequency to reduce the increase of temperature and ensure a reproducible measurement of material characteristics for determining S-N curves [8,9]. However, this approach is based solely on adjusting the frequency to keep the temperature between defined maximum and minimum values instead of considering the strain rate. This leads to limitations regarding reproducibility of the determination of material properties. In addition, further limitations result with respect to the scope of application, since environmental conditions such as elevated and low temperature cannot be applied in situ.

The aim of this study is to develop a method which combines stress-controlled cyclic testing with throughout constant strain rate, regardless of the existing stress amplitude or incurring damage mechanisms. Therefore, this study deals with a scientific comparison of the characteristic-related effects of a constant and a varying strain rate by analyzing measurement parameters.

## 2 MEASUREMENT PARAMETERS

Strain rate dependency of composites has been exemplary proofed under quasi-static loading [10] and in fatigue investigations under multiple frequencies [11]. To determine the strain rate dependency of GFR-PU the measurands of dynamic Young's modulus ( $E_{dyn}$ ) and loss energy ( $W_1$ ) were recorded and will be explained in the following.

### 2.1 Dynamic Young's modulus

Dynamic Young's modulus can be described by the gradient of a linear slope between the reversal points of a hysteresis loop (Fig. 1a). Under cyclic loading, the dynamic Young's modulus represents material stiffness, which usually shows a decreasing trend and is commonly used for modeling the damage state and for lifetime prediction.

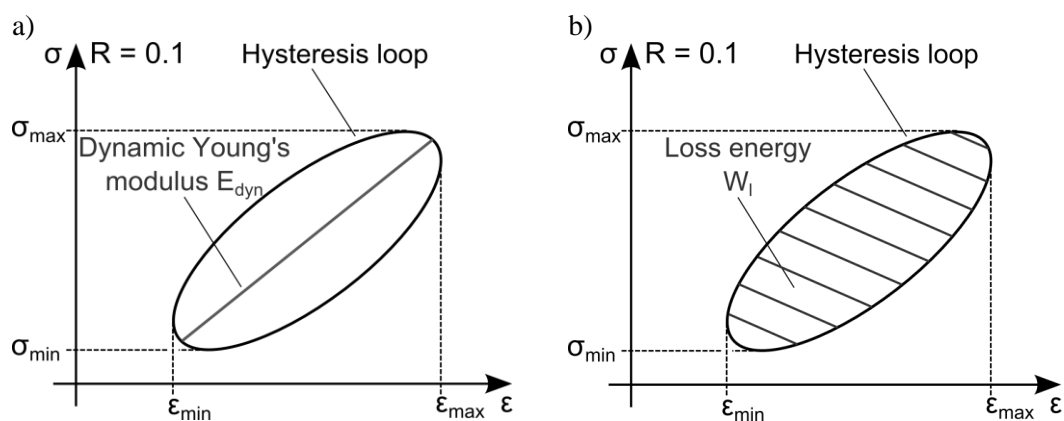


Figure 1: a) Dynamic Young's modulus and b) loss energy measured by hysteresis loop.

## 2.2 Loss energy

Loss energy is defined as the area of the enclosed hysteresis loop (Fig. 1b) and represents the dissipated energy during a load cycle [12]. The energy dissipation is based mostly on internal friction, which results in specimen heating. Thereby a correlation between loss energy and change in specimen temperature is suitable. Furthermore, damage development results in an increase of loss energy, because the material loses the property to return the energy.

## 3 MATERIAL

A two-component polyurethane thermosetting system (2K-PU) was chosen for HP-RTM process. The 2K-PU can be adjusted by adding a catalyst to the polyol component to increase its reactivity depending on the size of the desired part. The PU includes an internal release agent. The multilayer reinforcement was a 16-layers quasi-isotropic  $[45/-45/0/90/45/-45/0/90]_s$  glass-fiber satin weave setup with a surface area weight of  $300 \text{ g/m}^2$ . The fabric is coated with a PU compatible sizing TF970 from Hexcel. In Table 1 resin properties are listed.

Designation	Polyurethane	
Young's modulus	[GPa]	3.1
Tensile strength	[MPa]	62.8
Fracture strain	–	$9.1 \cdot 10^{-2}$
Glass transition temperature	[°C]	130 (DSC)

Table 1: Resin properties of polyurethane.

For the HP-RTM process, a high-pressure mixing system (Isotherm PSM90) with self-cleaning mixing head (GP600) is connected to the project-specified designed plate tool visualized in Fig. 2. The injection port is located on the lower mold in the vertical direction. The preform is placed in the preheated mold ( $85 \text{ }^\circ\text{C}$ ) and compressed to a plate thickness of 4 mm. The applied vacuum of 0.8 bar increases the impregnation and therefore mechanical properties during injection [13]. Two sensors (Kistler 6161A) monitor cavity pressure during the process. The PU resin is injected within 41 s with an injection rate of 7 g/s for accurate part quality. For this HP-RTM process, a cavity pressure of 45 bars was measured and a fiber volume fraction of 46% was determined. After the HP-RTM process, the plates were tempered for 7 hrs. at  $120 \text{ }^\circ\text{C}$  to optimize the mechanical properties. Afterward, the specimens were processed using water jet cutting. The specimen's geometry was chosen as defined in DIN527-4 1B with a total length of 180 mm. [3]

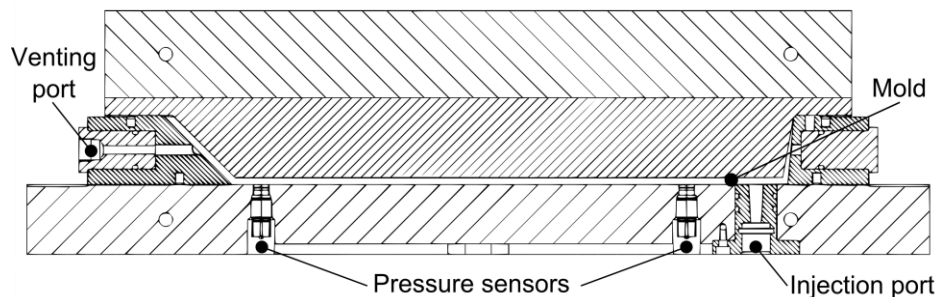


Figure 2: Section through RTM tool. [3]

## 4 EXPERIMENTAL PROCEDURES

### 4.1 Testing procedures

Instrumented multiple amplitude tests (MAT) were performed stress-controlled at servo-hydraulic testing system (Instron 8801,  $F_{\max} = \pm 100 \text{ kN}$ ) under tension-tension loading, load ratio  $R = 0.1$ , using sinusoidal load-time functions at room temperature. MAT exhibit the opportunity of efficient

estimation of the fatigue properties for various materials and has been successfully applied to FRP in previous studies [2,3]. As schematically displayed in Fig. 3a, the maximum stress amplitude  $\sigma_{\max}$  is increased stepwise from  $\sigma_{\max,\text{start}} = 20$  MPa each  $\Delta N = 10^4$  cycles by  $\Delta\sigma_{\max} = 20$  MPa until failure. The material response was detected during the test. The results have been exemplarily validated in constant amplitude tests (CAT) at  $\sigma_{\max} = 140$  MPa (Fig. 3b), which will be presented in further publications.

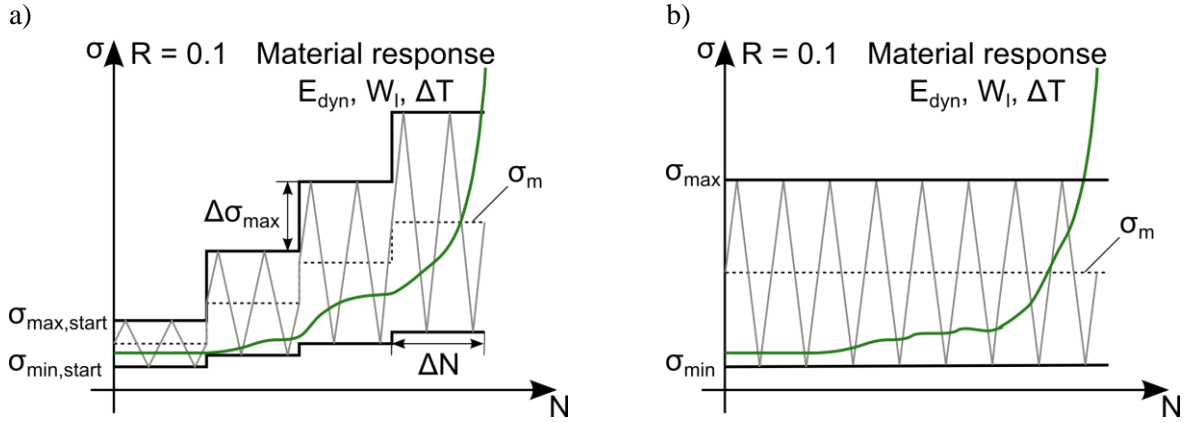


Figure 3: a) Scheme of multiple amplitude test (MAT) and b) constant amplitude test (CAT).

## 4.2 Frequency adjustment

With the use of conventional soft- and hardware a direct strain rate adjustment isn't possible under stress-controlled loading. Thus, in order to realize indirect strain rate adjustment, the stress rate had been kept constant by varying frequency. It can be seen in Fig. 4a that the stress rate (similar to strain rate for linear-elastic material behavior) is different for both curves due to varying stress amplitudes, whereas in Fig. 4b, proven by  $\alpha$ , an approximately similar stress rate and thereby strain rate can be realized by adjusting the cycle time ( $t_{r2} > t_{r1}$ ). Adapted frequency leads to a change in the cycle time of a sinusoidal oscillation, which in this case results in a constant strain rate for unchanged elastic material properties.

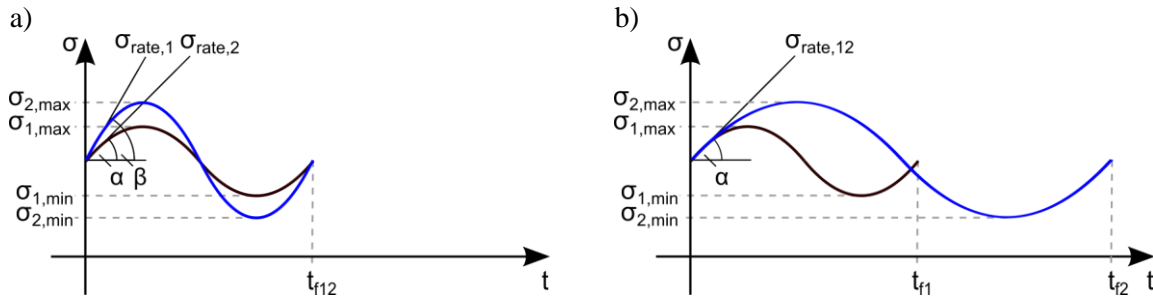


Figure 4: a) Different stress rates at equal cycle time due to varying maximum stress and b) constant stress rate due to adjusted cycle time respectively frequency.

$$\Delta\sigma_{t,i} = 4 \cdot \sigma_{a,i} \quad (1.1)$$

$$\sigma_{\text{rate},\text{start}} = \Delta\sigma_{t,\text{start}} \cdot f_{\text{start}} \quad (1.2)$$

$$f_{\text{ad},i} = \sigma_{\text{rate},\text{start}} \cdot \Delta\sigma_{t,i}^{-1} \quad (1.3)$$

In order to realize a constant stress rate during the tests the frequency for each step of MAT has been calculated with regard to equation 1.1 to 1.3. The summarized delta in stress for a sinusoidal loop of each step  $\Delta\sigma_{t,i}$  can be defined by the corresponding stress amplitude  $\sigma_{a,i}$  multiplied by 4 (equation

1.1). For the first step this results in  $\Delta\sigma_{t,start} = 36$  MPa. In equation 1.2 solely the stress rate of the first step  $\sigma_{rate,start}$  is calculated by multiplying  $\Delta\sigma_{t,start}$  and  $f_{start}$  (10 Hz). In the further course, equation 1.3 can be applied for defining the adjusted frequency for each step  $f_{ad,i}$  by dividing  $\sigma_{rate,start}$  with the corresponding  $\Delta\sigma_{t,i}$ . It is noted that equations 1.1 to 1.3 assume a constant stress rate within a sinusoidal loop, whereas in effect a cosinusoidal behavior appears. In Table 2 the resulting adjusted frequencies are listed, which have been used in present investigations.

Maximum stress $\sigma_{max}$ [MPa]	Adjusted frequency $f_{ad}$ [Hz]	Maximum stress $\sigma_{max}$ [MPa]	Adjusted frequency $f_{ad}$ [Hz]
20	10.0	120	1.7
40	5.0	140	1.4
60	3.3	160	1.3
80	2.5	180	1.1
100	2.0	200	1.0

Table 2: Adjusted frequencies for MAT with  $\Delta\sigma_{max} = 20$  MPa.

### 4.3 Measurements

For the investigation of the cyclic deformation behavior of GFR-PU, the material response in terms of dynamic Young's modulus, loss energy, and temperature has been detected. In this context, strain measurements for hysteresis measurements were performed with an extensometer (Instron,  $l_0 = 50$  mm,  $\Delta l = \pm 5$  mm). Dynamic Young's modulus was calculated in accordance with equation (2). The temperature was measured with thermocouples at three positions on specimen's surface as well as a reference temperature representing room temperature. The experimental setup is shown in Fig. 5.

$$E_{dyn} = (\sigma_{max} - \sigma_{min}) \cdot (\epsilon_{max} - \epsilon_{min})^{-1} \quad (2)$$

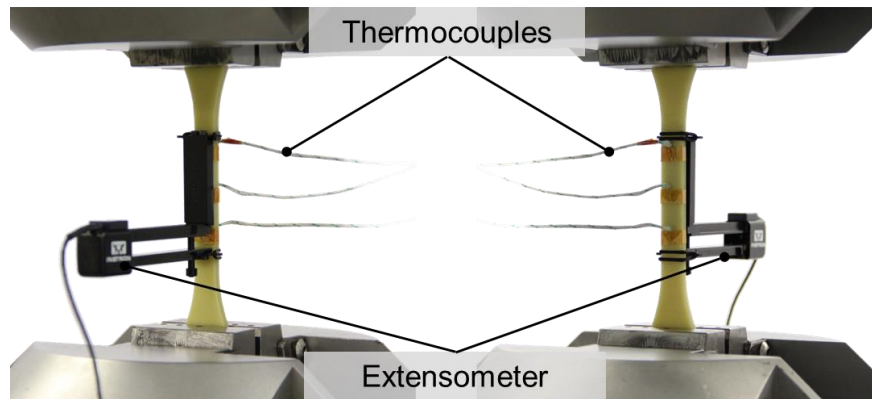


Figure 5: Experimental setup for cyclic investigations.

Strain rate is calculated by a self-developed LabView program to assess the accuracy of the frequency adjustment with regard to the strain rate. The LabView program detects approximately 100 points per loop (for  $f = 10$  Hz). For each point, the derivative of the amount is calculated and the average of strain rate is defined for the corresponding cycle. Each 100 cycles, the adjusted frequency is calculated which would result in a constant strain rate despite non-elastic material behavior. Therefore, the calculated cycle-specific average of strain rate is applied to equations 1.1 to 1.3.

## 5 RESULTS

In Fig. 6 results are presented for MAT for both constant and adjusted frequencies. The curve  $\sigma_{\max}$  shows the stepwise increase of maximum stress until failure at 200 MPa. The strain rate is displayed as a function of number of cycles  $N$  and related to maximum stress  $\sigma_{\max}$  and constant frequency (Fig. 6a) respectively adjusted frequencies (Fig. 6b). For constant frequency of 10 Hz, the strain rate increases with each step and furthermore within one step occurring firstly at  $\sigma_{\max} = 100$  MPa. This behavior steadily expands related to the maximum stress and results in an overall increase of the strain rate about 1.400%. This trend can be avoided by frequency adjustment with respect to Table 2 (Fig. 6b). The results show great differences compared to a constant frequency, represented by a small increase of strain rate of approximately 38%. However, it can be noted that constant stress rate due to adjusted frequency doesn't lead to a continuously constant strain rate.

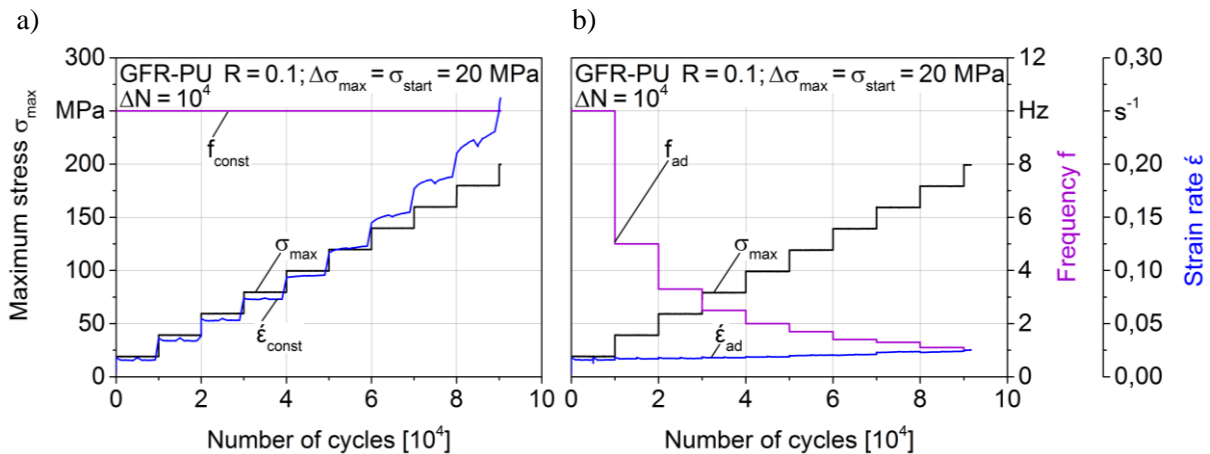


Figure 6: Multiple amplitude test (MAT) with a) constant frequency and b) adjusted frequencies.

In order to compare the change in strain rate solely resulting out of a change in material properties, the test data of the MAT with constant frequency were edited. Particularly, the absolute changes in strain rate have been deleted afterwards, which occur during the shift from one step to another due to the increase in  $\sigma_{\max}$ . This leads to a curve for strain rate  $\dot{\epsilon}_{\text{const,cal}}$ , which represents the absolute increase in strain rate within the steps of the MAT for constant frequency. In Fig. 7 this curve is compared to the strain rate for adjusted frequency  $\dot{\epsilon}_{\text{ad}}$  already described in Fig. 6b. A relevant difference occurs starting at  $\sigma_{\max} = 120$  MPa, which expands continuously until failure.

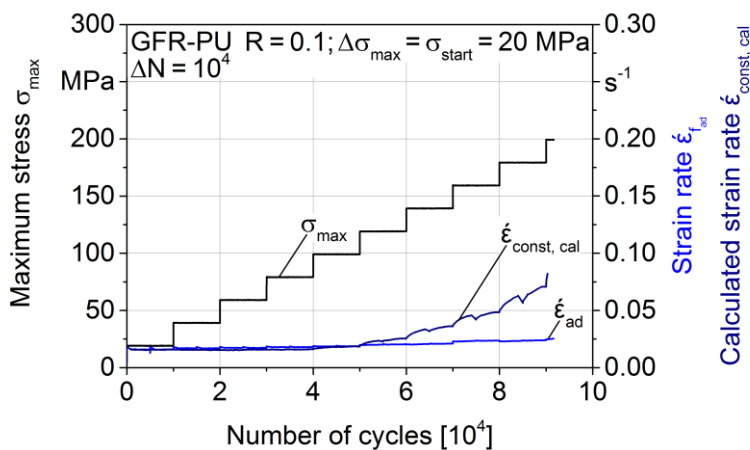


Figure 7: Comparison of strain rate development within the steps for constant frequency and adjusted frequencies.

The comparison of the developments of change in temperature  $\Delta T$  and loss energy  $W_I$  for constant frequency and adjusted frequencies with regard to the afore-explained MAT is shown in Fig. 8a-b. The measurands are plotted as function of number of cycles  $N$  corresponding to maximum stress  $\sigma_{max}$ . Loss energy  $W_I$  is increasing stepwise depending on maximum stress development. However, the stepwise increase shows a disproportionately behavior, increasing with each step. Within one step, loss energy stays nearly constant until 180 MPa maximum stress, which leads to a rapid increase of  $W_I$  until failure at approx. 0.40 J for constant frequency. For adjusted frequency, loss energy shows a similar behavior, whereas the absolute values are about 10% below the values at constant frequency during the whole procedure. Instead, the evolution of change in temperature shows significant differences for both methods. The temperature increases already at 60 MPa maximum stress for constant frequency. At failure change in temperature is approximately 35 K, while change in temperature for adjusted frequency is approximately 5 K. In comparison, an increase of 5 K for change in temperature at a constant frequency is already reached at 100 MPa maximum stress. The great difference in temperature correlates with the increase in energy rate for the constant frequency with every step compared to the adjusted frequency. The energy dissipation is mostly based on internal friction, which thereby leads to an increase in temperature. However, an oscillating development in the change in temperature for the entire test can be detected in each step. This behavior is due to a new intermitting method of stiffness measurement in included tensile tests, which doesn't influence the mechanical behavior, but leads to specimens cooling [14].

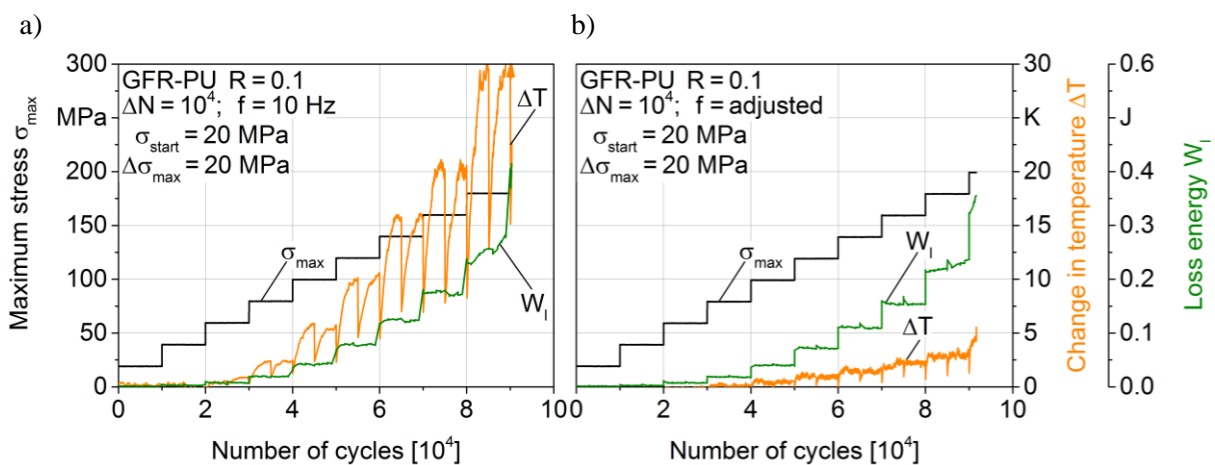


Figure 8: Change in temperature for MAT with a) constant frequency and b) adjusted frequencies.

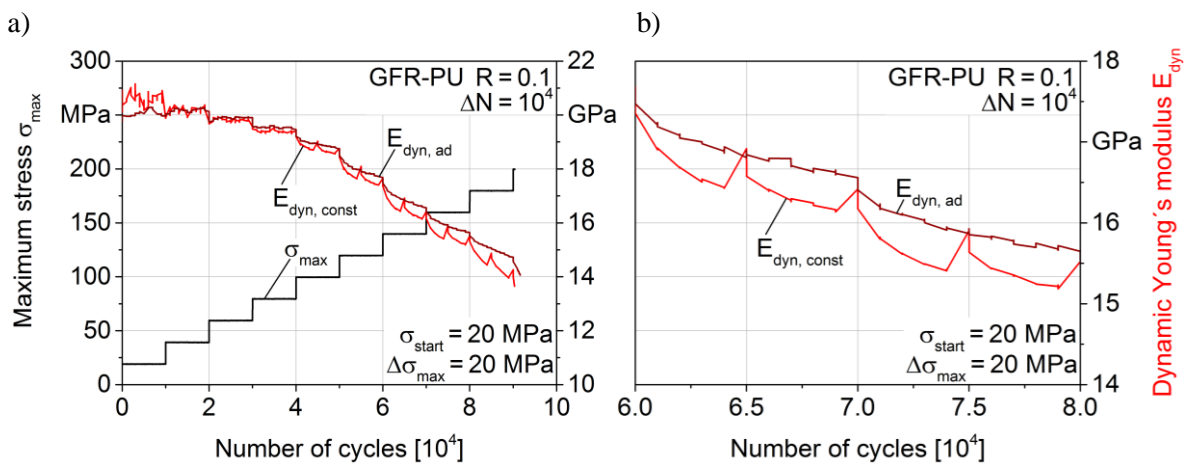


Figure 9: Comparison of dynamic Young's modulus development for constant and adjusted frequencies a) for the whole MAT and b) with higher magnification for  $\sigma_{max} = 140$  and 160 MPa

In Fig. 9a the developments of  $E_{\text{dyn}}$  of aforementioned MAT are displayed.  $E_{\text{dyn, const}}$  represents the results of the MAT with the constant frequency, whereas  $E_{\text{dyn, ad}}$  illustrates the results of the MAT with adjusted frequencies. Because of computing limitations measuring points were taken and calculated all 100 cycles via LabView. While both curves show a similar digressive trend, in contrast to  $E_{\text{dyn, const}}$ ,  $E_{\text{dyn, ad}}$  doesn't decrease until  $\sigma_{\text{max}} = 60$  MPa. In both cases, at the end of each step,  $E_{\text{dyn}}$  shows a lower value compared to step's beginning. The residual stiffness is approximately 66% for  $E_{\text{dyn, const}}$  and 70% for  $E_{\text{dyn, ad}}$ , which indicates the influence of frequency respectively strain rate on the stiffness degradation. Furthermore, dynamic Young's modulus shows smaller drops in absolute values for adjusted frequency, which is paradoxical regarding the relationship of stiffness and strain rate under quasi-static loading [15]. In the case of cyclic testing, this paradox can be explained by the influence of temperature on mechanical properties, since increasing temperature (Fig. 8a-b) leads to decreasing stiffness [16]. Fig. 9b gives an in-depth view in differences between the stiffness developments exemplarily for  $\sigma_{\text{max}} = 140$  and 160 MPa. Adjusted frequencies lead to a more homogenous decrease of  $E_{\text{dyn, ad}}$  in comparison to  $E_{\text{dyn, const}}$ . Starting at  $\sigma_{\text{max}} = 60$  MPa,  $E_{\text{dyn, const}}$  shows a periodic increase in the end of each step, followed by a subsequent decrease. It is likely that this behavior is due to the included tensile tests (each  $5 \cdot 10^3$  cycles), which lead to a cooling of the specimen (see oscillating temperature in Fig. 8a) and thereby to an increase in stiffness. In the following, the temperature again increases under cyclic loading especially after shifting to the next step (each  $10^4$  cycles), which results in a decrease in stiffness. With regard to modeling approaches based on stiffness degradation, it has to be mentioned that an unsuitable strain rate seems to lead to a deviation in stiffness, which hinders the development of a proper model.

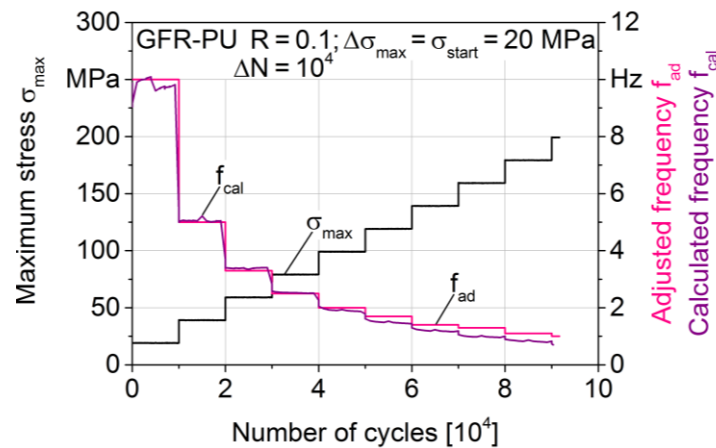


Figure 10: Comparison of adjusted frequencies (Table 2) and calculated frequencies (LabView).

The investigations prove that for adjusted frequencies respectively a constant stress rate, the measurands change in temperature and dynamic Young's modulus show different evolutions compared to a constant frequency. It has to be mentioned that the present approach of adjusted frequencies is based on an assumption of a complete linear-elastic stress-strain behavior of the material. However, occurring damages, as well as specimen heating, lead to a non-elastic behavior, which results in a change in strain rate despite constant stress rate. For this reason, a previous frequency adjustment on the basis of elastic material behavior isn't suitable to ensure a steady constant strain rate. In order to achieve the needed accuracy regarding constant strain rate the LabView program was applied, which calculates the required frequencies based on the measured hysteresis loops each 100 cycles. The adjusted frequencies (Table 2) and the calculated frequencies (LabView) are compared in Fig. 10. Both curves decrease stepwise every step. Based on the mentioned non-elastic stress-strain behavior the calculated frequencies show a disproportionately degrading trend in every following step starting at  $\sigma_{\text{max}} = 100$  MPa. The differences between the adjusted frequency and calculated frequency confirm the necessity to generate an in-situ control that allows a constant strain rate by instantly adjusting the frequency.

## 6 CONCLUSIONS AND OUTLOOK

With the aim of investigating the strain rate influence on mechanical characteristic values of GFR-PU, instrumented multiple amplitude tests were carried out applying two approaches: i) constant frequency and ii) adjusted frequencies to realize constant stress rate (similar to constant strain rate for linear elastic material behavior). After analyzing specific measurands of the testing results, following findings can be specified:

**Strain rate** development shows to be great influenced by stress rate and frequency, respectively. This is proofed by significantly lower increase in strain rate for adjusted frequencies despite eliminating the stress-specific increase in strain rate for constant frequency.

**Loss energy** exhibits a similar development for both approaches with minor differences, which indicate that this measurand seems to be less affected by changes in strain rate.

**Change in temperature** shows a significant increase similar to a potential gradient for constant frequency, whereas in comparison a constant strain rate results in a drastic reduction in the change in temperature of about 85%.

**Dynamic Young's modulus** shows a more homogenously decrease for adjusted frequencies compared to a constant frequency. Therefore, an unsuitable strain rate seems to lead to a deviation in stiffness, which has to be considered for development of a proper model in context with lifetime prediction.

With regard to the results, it should be noted that no continuously constant strain rate could be realized due to the applied approach, which is based on an assumption of a steady linear elastic behavior. The (calculated) frequencies determined with use of a self-developed LabView software show that the strain rate changes differently, which can be explained by non-elastic mechanisms as for example specimen heating and damages. This demonstrates the need for an optimized test method, in which a constant strain rate adaptation is achieved by means of the temporally present strain rate. In this context, the authors are currently investigating a method in which an evaluation of the current strain rate is carried out on the basis of hysteresis measurements and furthermore on a subsequent adaptation of the frequency. This allows the compensation of the material specific strain rate dependency and thereby a reproducible determination of the material characteristics is realized.

## ACKNOWLEDGEMENTS

The authors thank the Federal Ministry for Economic Affairs and Energy (BMWi) for the funding of the research project "PRISCA" (code KF2198131) as well as the Commission for Technology and Innovation (CTI) for supporting the partners from Switzerland in this EUREKA research project. The excellent collaboration with all project partners is gratefully acknowledged.

## REFERENCES

- [1] J. Fan, J. Njuguna, An introduction to lightweight composite materials and their use in transport structures, J. Njuguna (Ed.), *Lightweight Composite Structures in Transport*, 1st Ed., Woodhead Publishing, 2016, pp. 3-34.
- [2] F. Walther, Microstructure-oriented fatigue assessment of construction materials and joints using short-time load increase procedure, *Materials Testing* **56**, 2014, pp. 519-527 (doi: 10.3139/120.110592).
- [3] D. Huelsbusch, M. Jamrozy, G. Frieling, Y. Mueller, G.-A. Barandun, M. Niedermeier and F. Walther, Comparative characterization of quasi-static and cyclic deformation behavior of glass fiber-reinforced polyurethane (GFR-PU) and epoxy (GFR-EP), *Materials Testing* **59**, 2017, pp. 109-117 (doi: 10.3139/120.110972).
- [4] M. Schoßig, C. Bierögel, W. Grellmann, T. Mecklenburg, Mechanical behavior of glass fibre reinforced thermoplastic materials under high strain rates, *Polym. Test.* **27**, 2008, pp. 893-900 (doi: 10.1016/j.polymertesting.2008.07.006).

- [5] R. O. Ochola, K. Marcus, G. N. Nurick, T. Franz, Mechanical behaviour of glass fibre reinforced composites at varying strain rates, *Compos. Struct.* **63**, 2004, pp. 455-467 (doi: 10.1016/S0263-8223(03)00194-6).
- [6] J. M. L. Reis, J. L. V. Coelho, A. H. Monteiro, H. S. da Costa Mattos, Tensile behavior of glass/epoxy laminates at varying strain rates and temperatures, *Compos. Part. B-Eng.* **43**, 2012, pp. 2041-2046 (doi: 10.1016/j.compositesb.2012.02.005).
- [7] Y. Ou, D. Zhu, Tensile behavior of glass fibre reinforced composite at different strain rates and temperatures, *Constr. Build. Mater.* **96**, 2015, pp. 648-656 (doi: 10.1016/j.conbuildmat.2015.08.044).
- [8] J. Brunbauer, H. Stadler, G. Pinter, Mechanical properties, fatigue damage and microstructure of carbon/epoxy laminates depending on fibre volume content, *Int. J. Fatigue.* **70**, 2015, pp. 85-92 (doi: 10.1016/j.ijfatigue.2014.08.007).
- [9] H. Zilch-Bremer, Frequency/Temperature-controlling, *Hysteresis-Measurements*, (Original German title: Frequenz/Temperatur-Regelung, *Hysteresis-Meßverfahren*), Lehrstuhl für Kunststofftechnik, 1993, pp. 3.2.1-3.2.6
- [10] M. M. Shokrieh, M. J. Omid, Tension behavior of unidirectional glass/epoxy composites under different strain rates, *Compos. Struct.* **88**, 2009, pp. 595-601 (doi: 10.1016/j.compstruct.2008.06.012)
- [11] M. Fray, V. Altstädt, Fatigue behaviour of multiblock thermoplastic elastomers. 3. Stepwise increasing strain test of poly(aliphatic/aromatic-ester) copolymers, *Polymer.* **45**, 2004, pp. 263-273 (doi: 10.1016/j.polymer.2003.10.034)
- [12] B. von Bernstorff, G.W. Ehrenstein, Failure mechanism in SMC subjected to alternating stresses, *J. Mater. Sci.* **25**, 1990, pp. 4087-4097.
- [13] R. Chaudhari, P. Rosenberg, M. Karcher, S. Schmidhuber, P. Elsner and F. Henning, High-pressure RTM process variants for manufacturing of carbon fiber-reinforced composites, *Proceedings of the 19<sup>th</sup> International Conference on Composite Materials ICCM19, Montreal, Canada, 2013, July 28 - August 2*, pp. 1-9.
- [14] J. Brunbauer, F. Arbeiter, S. Stelzer, G. Pinter, Stiffness based fatigue characterization of CFRP, *Adv. Mat. Res.* **891-892**, 2015, pp. 166-171
- [15] S. R. Raisch and B. Möglinger, High rate tensile tests – Measuring equipment and evaluation, *Polym. Test.* **29**, 2010, pp. 265-272 (doi: 10.1016/j.polymertesting.2009.11.010).
- [16] Z. Lu, G. Xian, H. Li, Effects of elevated temperatures on the mechanical properties of basalt fibers and BFRP plates, *Constr. Build. Mater.* **127**, 2016, pp. 1029-1036, (doi: 10.1016/j.conbuildmat.2015.10.207).